

---

# Preparation and Characterization of Carbon Nanofibers and its Composites by Chemical Vapor Deposition

---

Chang-Seop Lee and Yura Hyun

Additional information is available at the end of the chapter

<http://dx.doi.org/10.5772/63755>

---

## Abstract

Hydrocarbon gas or carbon monoxide was pyrolyzed by chemical vapor deposition (CVD), and carbon nanofiber (CNF) synthesis was performed using transition metals such as Ni, Fe, and Co as catalysts. When synthesizing carbon nanofibers using the CVD method, experimental variables are temperature, catalysts, source gas, etc. Especially, the particle size of the catalyst is the most important factor in determining the diameter of carbon nanofibers. Hydrocarbon gases, such as  $\text{CH}_4$ ,  $\text{C}_2\text{H}_4$ , benzene, and toluene are used as the carbon source, and in addition to these reaction gases, nonreactive gases such as  $\text{H}_2$ , Ar, and  $\text{N}_2$  gases are used for transportation. Synthesis occurs at a synthesis temperature of 600–900°C, and catalyst metals such as Ni, Co, and Fe are definitely required when synthesizing CNFs. Therefore, it is possible to synthesize CNFs in selective areas through selective deposition of such catalyst metals. In this study, CNFs were synthesized by CVD. Ethylene gas was employed as the carbon source for synthesis of CNFs with  $\text{H}_2$  as the promoting gas and  $\text{N}_2$  as the balancing gas. Synthesized CNFs can be used in various applications, such as composite materials, electromagnetic wave shielding materials, ultrathin display devices, carbon semiconductors, and anode materials of Li secondary batteries. In particular, there is an increasing demand for light-weight, small-scale, and high-capacity batteries for portable electronic devices, such as notebook computers or smartphones along with the recent issue of fossil energy depletion. Accordingly, CNFs and their silicon-series composites are receiving attention for use as anode materials for lithium secondary batteries that are eco-friendly, light weight, and high capacity.

**Keywords:** carbon nanofibers, transition metal catalyst, chemical vapor deposition, composite, Li ion batteries

## 1. Introduction

Chemical vapor deposition (CVD) is widely used as a surface treatment technology for materials. CVD forms a solid-state thin film mostly on the surface and is used not only to produce high-purity bulk materials and powder but also to manufacture composite materials through infiltration techniques.

CVD is used to deposit a wide variety of materials. Most of the elements in the periodic table deposited in the pure element are formed by CVD technology. However, they are deposited mostly in the compound form rather than the pure element form. CVD can make precursor gases flow to one or more heated objects in a chamber to coat the desired compound. A chemical reaction occurs on the hot surface, and this leads to the deposition of a thin film on the surface. This reaction also produces the unreacted precursor gas and the chemical byproduct discharged from the chamber at the same time.

CVD can deposit many kinds of materials and can be applied to broad areas, so the synthesis condition is also diverse. CVD synthesis can occur in a high- or low-temperature reactor, the pressure ranges from sub-Torr pressures to above-atmospheric pressures, regardless of the kind of catalyst, and the reaction temperature can range from 200 to 1600°C to diversify the synthesis condition.

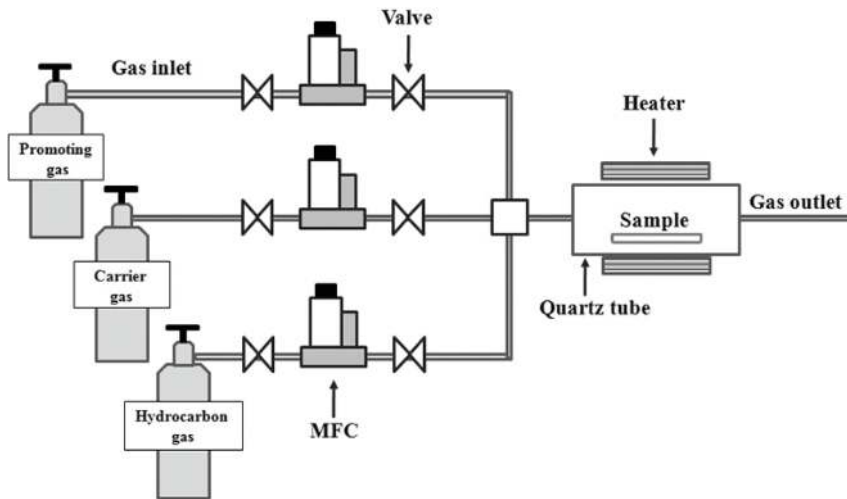


**Figure 1.** The schematic diagram of a tube-furnace CVD system.

Microfabrication processes widely use CVD to deposit materials in various forms, including monocrystalline, polycrystalline, amorphous, and epitaxial. These materials include silicon ( $\text{SiO}_2$ , germanium, carbide, nitride, and oxynitride), carbon (fiber, nanofibers, nanotubes, diamond, and graphene), fluorocarbons, filaments, tungsten, and titanium nitride [1, 2].

CVD is a technology used to deposit a solid-state thin film on the substrates from vapor species through chemical reaction. One of the most unique characteristics of CVD synthesis is that chemical reaction plays an important role, so it is comparable to other thin film deposition technologies. **Figure 1** shows the schematic drawing of a typical tube-furnace CVD system. Gas flows are regulated by mass flow controllers (MFCs) and fed into the reactor through a gas-distribution unit. Chemical deposition takes place in the reactor, which is heated by outside heaters.

During the CVD process, the reaction gas is supplied to the reactor through mass flow controllers (MFCs) controlling the flow rate of the gas being passed. In addition, the mixture gas device mixes the gases evenly before they flow into the reactor. The chemical reaction occurs in the reactor and solid-state materials are deposited on the substrates. A heater is placed around the reactor to provide reaction at high temperatures. CVD is used not only to create a solid-state thin film on the surface and produce high-purity bulk materials and powder but also to manufacture composite materials through infiltration techniques. CVD is used to deposit various materials on solid surfaces.

A characteristic feature of CVD technique is its excellent throwing power, enabling the production of coatings of uniform thickness and properties with low porosity even on substrates with complicated shapes. Another characteristic feature is the possibility of localized or selective deposition on patterned substrates [1–4].

In this chapter, we describe the preparation process for carbon nanofibers (CNFs) and their silicon/silicon oxide composites using the chemical vapor deposition method and investigate the physicochemical and electrochemical characteristics of the prepared materials for the application of anode materials in Li secondary batteries.

## **2. Synthesis and characterization of CNFs on transition metal catalysts by CVD**

### **2.1. Preparation of transition metal catalysts**

In this study, transition metal catalysts were prepared through the coprecipitation method and then used in the synthesis of CNFs. In order to prepare the metal catalysts with different compositions, the mass of the precursor was first calculated according to the ratio of the metal content required.

Solution A was composed of aluminum nitrate, which helps to generate alumina ( $\text{Al}_2\text{O}_3$ ) to serve as a supporter for the transition metal catalysts in the transition metal nitrate, dissolved in distilled water. With the foregoing supporter working to capture the nanometal catalyst, the coagulation phenomenon occurs when the temperature is increased up to the temperature for the synthesis of carbon nanofibers without a supporter because of the unstable nanometal particles. The usage of a supporter helps carbon nanofibers grow without a clustered catalyst and thereby serves as a matrix that prevents catalyst coagulation.

Meanwhile, it is preferred to mix passive metals to control the interparticle coagulation of transition metals, such as Fe, Co, and Ni, which all have catalytic activity against the reaction gas during high-temperature reaction. This study employed a mixture of the foregoing Solution A and another Solution B, which was composed of ammonium molybdate and distilled water.

Solution C was made of ammonium carbonate, which served as a precipitator to precipitate the transition metals and the aluminum included in the foregoing Solution A. Precipitation was induced by gradual blending of the mixture composed of Solutions A and B and the mixture of Solution C. This step was followed by agitation for stability of the precipitation.

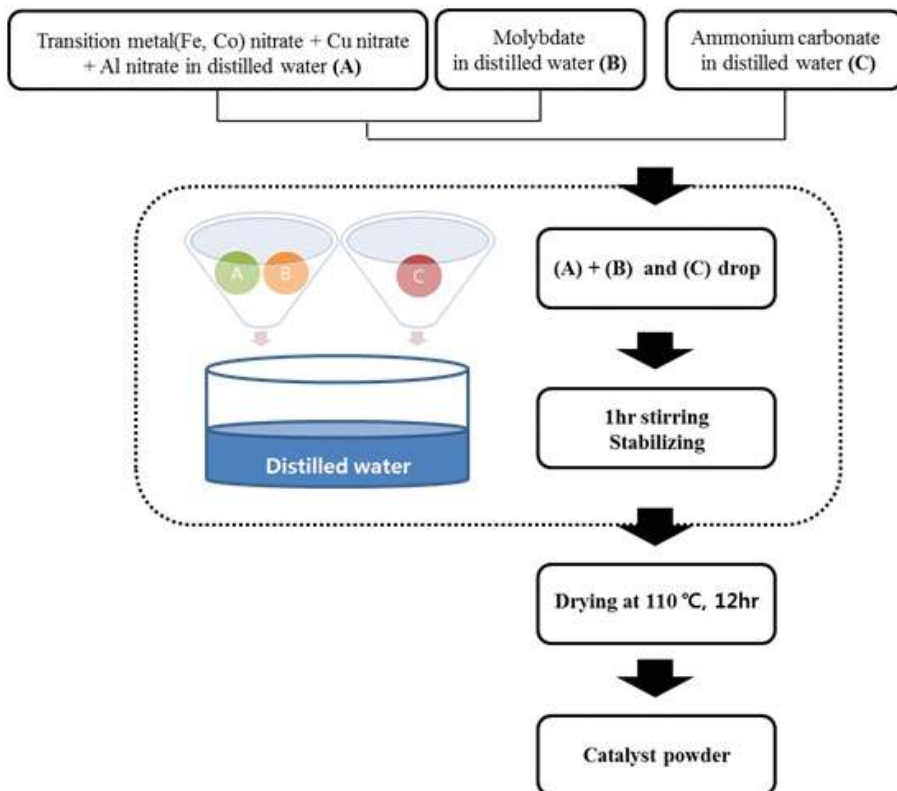


**Figure 2.** Preparation process transition metal catalysts.

These solutions were sufficiently stirred to stabilize the precipitates; moisture was removed by filtering; and they were dried for more than 12 h in a 110°C oven. Fully dried precipitates were made into powder, and this powder of a metal catalyst was used as the catalyst in the synthesis of carbon nanofibers. The preparation process for the catalysts is shown in **Figure 2** [5–13].

## 2.2. Synthesis of CNFs

Chemical vapor deposition (CVD) method was employed to synthesize carbon nanofibers in horizontal tube furnace. The schematic diagram of the reaction apparatus, manufactured as metal heating element and horizontal quartz reaction tube in 80 mm (diameter) × 1400 mm (length), was demonstrated in **Figure 3**.

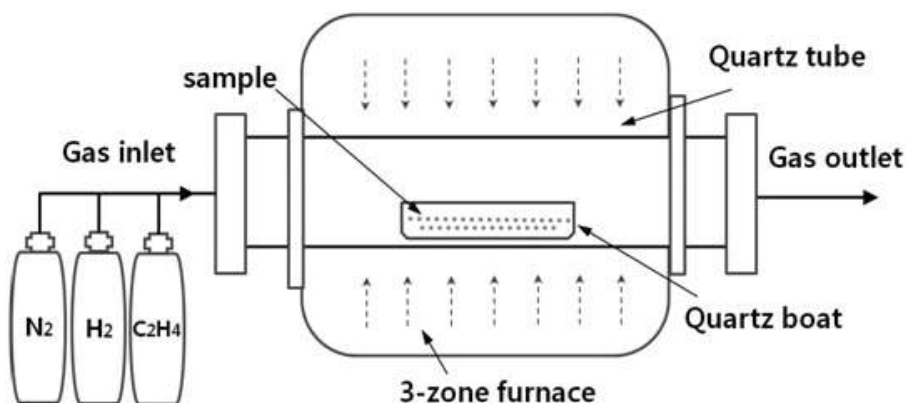


**Figure 3.** Schematic diagram of CVD apparatus for preparation of CNFs.

Flux of reaction gas was regulated by electronic mass flow controller (MFC); ethylene gas ( $C_2H_4$ ) was used to grow carbon nanofibers; and  $2H_2$  gas was used as promoting gas for gas phase reaction, whereas  $N_2$  gas was used for stabilization of reaction. Following are conditions of synthesis reaction.

A prepared metal catalyst was evenly spread on a quartz boat, placed into reactor under  $N_2$  atmosphere, and temperature was increased to  $10^\circ C/min$ . When the temperature was reached  $700^\circ C$ , it was maintained for 30 min; 20%  $H_2$  gas balanced with  $N_2$  gas were flown into all together; and then  $H_2$  gas balanced with  $N_2$  gas and 20% ethylene balanced with  $N_2$  gas were flown into the reactor for 1 h. Ethylene and  $H_2$  gas were shut off after the reaction was completed;  $N_2$  gas was passed with the reactor atmosphere inactive until room temperature was reached. Then, carbon nanofibers were synthesized [11, 14, 15].

## 2.3. Synthesis of CNFs on iron and copper catalysts

### 2.3.1. Scanning Electron Microscope (SEM)

Carbon nanofibers are synthesized when pyrolyzed hydrocarbons contact metal particles at high temperature. The microstructure of the synthesized carbon nanofibers was observed by SEM and is shown in **Figure 4**. As shown in **Figure 4(a)–(d)**, carbon nanofibers grew both in

the case of synthesis by Fe catalyst only as well as with an Fe:Cu weight ratio of 7:3, 5:5, and 3:7. In addition, it is known that the fiber diameters average 25–35 nm. Since physical properties may vary depending on diameter size, the diameters of carbon nanofibers can be adjusted according to the weight ratio of catalysts to meet specific purposes.

It was found that the carbon nanofibers grew slightly in the SEM image in (e) but not in (f). Here, it is believed that Fe played the role of a positive catalyst, whereas Cu played the role of a negative catalyst [9, 11].

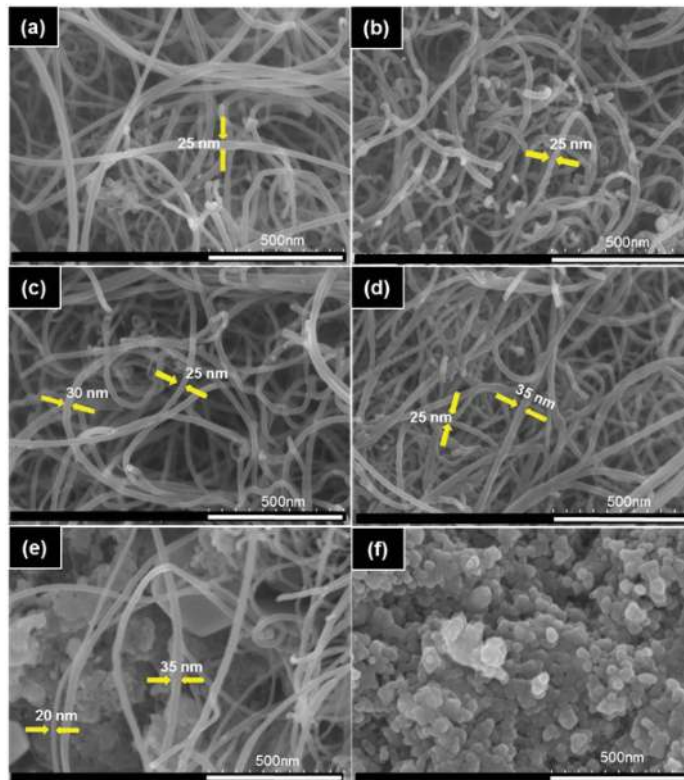


**Figure 4.** SEM images of CNFs synthesized from ethylene at 700°C under different concentrations of Fe and Cu catalysts. (a) Fe:Cu = 10:0, (b) Fe:Cu = 7:3, (c) Fe:Cu = 5:5, (d) Fe:Cu = 3:7, (e) Fe:Cu = 1:9, and (f) Fe:Cu = 0:10.

### 2.3.2. Brunauer–Emmett–Teller (BET)

A comparison was performed by measuring the surface area ( $\text{m}^2/\text{g}$ ) of respective carbon nanofibers using a measuring instrument for specific surface area. When the weight ratio of Fe and Cu was 3:7, the highest BET surface area was found to be 305  $\text{m}^2/\text{g}$ . With weight ratios of 289, 264, 250, and 77  $\text{m}^2/\text{g}$ , the respective BET surface areas were 10:0, 5:5, 7:3, and 1:9.

Synthesized carbon nanofibers usually have wide specific surface area, which makes them good at storing energy, and thus, they can be used as electrodes materials for capacitor or lead storage batteries, or lithium ion secondary batteries [8, 16].

### 2.3.3. X-ray Diffraction (XRD)

**Figure 5** shows the XRD results for the change of crystal quality according to the Fe and Cu weight ratio. It was confirmed that both carbon nanofibers synthesized with Fe catalyst only and those synthesized with Fe:Cu catalysts at the weight ratios of 7:3 and 5:5 showed carbon peaks with the highest strength.

Most carbon peaks had high strength except for the nanofibers synthesized with Fe and Cu at the weight ratio of 1:9. Therefore, the ratio of pure carbon nanofibers with excellent crystal quality was confirmed to be high [9, 11].

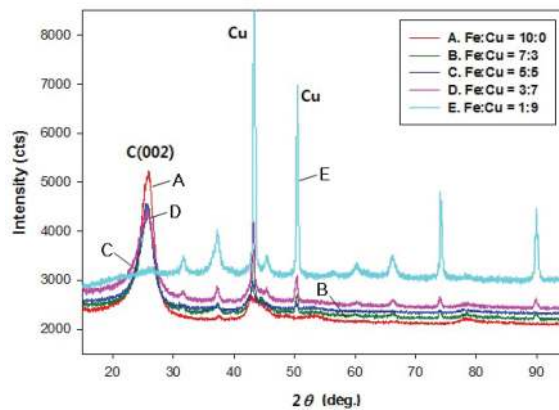


**Figure 5.** Change in carbon nanofiber crystal quality according to weight ratio of Fe and Cu.

## 3. Synthesis and characterization of SiO<sub>2</sub>/CNF composites by CVD

### 3.1. Synthesis and electrochemical performance of mesoporous SiO<sub>2</sub>-CNF composite on Ni foam

#### 3.1.1. Synthesis of catalysts and mesoporous SiO<sub>2</sub>

Binders, electronic conducting additives, and current collectors constituting the electrode are very important factors in the manufacturing process for batteries because the overall performance of the battery depends on the performance of these materials.

When the volume changes repeatedly during the adsorption and desorption of lithium, bonds of active materials become weaker or the conductive additives and contact resistance increase

in the electrode. In particular, because active materials such as silicon or tin are used in high-capacity electrodes, the volume changes are even bigger and thus the bond strength between the collector and the anode active materials become weaker.

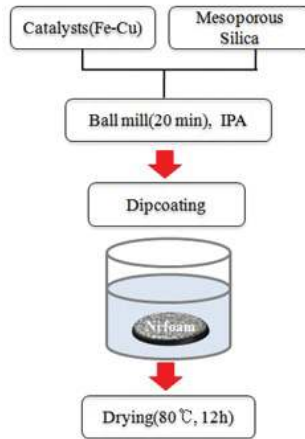


Figure 6. Deposition of catalysts and mesoporous SiO<sub>2</sub> on Ni foam.

Therefore, in this study, we tried to increase the bond strength between the collector and the anode active materials as well as to improve the problem regarding the volume expansion of the electrode by synthesizing CNFs and mesoporous SiO<sub>2</sub>-CNF composites directly on the collector, Ni foam, using the CVD method without a binder [17, 18] (Figure 6).

### 3.1.2. Synthesis of CNFs and mesoporous SiO<sub>2</sub>-CNF composites

CNFs and mesoporous SiO<sub>2</sub>-CNF composites were synthesized in the quartz reactor using chemical vapor deposition. The CVD apparatus used in this experiment is shown in Figure 7. C<sub>2</sub>H<sub>4</sub>/N<sub>2</sub>(20/80 vol%) gas was used as the carbon source for the synthesis of carbon nanofibers. H<sub>2</sub>/N<sub>2</sub>(20/80 vol%) and N<sub>2</sub>(99%) were used as the promotion gas for the gas phase reaction and the carrier gas, respectively.

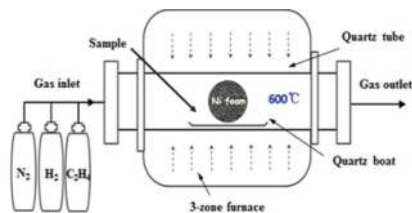


Figure 7. Schematic diagram of CVD apparatus for the preparation of CNFs and mesoporous SiO<sub>2</sub>-CNF composites.



After the Fe–Cu catalyst or Fe–Cu/mesoporous SiO<sub>2</sub> deposited on Ni foam was placed in the reaction furnace, the temperature was raised by 10°C/min while the nitrogen atmosphere was maintained. At 600°C, nitrogen and hydrogen gases were flowed while the temperature was maintained for 30 min. Hydrogen and ethylene gases were flowed for 10 min. After the reaction was completed, CNFs and mesoporous SiO<sub>2</sub>–CNF composites were synthesized by cooling to room temperature with nitrogen gas [17, 18].

### 3.1.3. Fabrication process of anode materials for lithium secondary batteries

A three-electrode cell was prepared by applying CNFs and mesoporous SiO<sub>2</sub>–CNF composites as anode active materials of lithium secondary batteries. Three-electrode cell was assembled in the glove box filled with Ar gas and was assembled as a half cell. The scheme for cell assembly is shown in **Figure 8**. Prepared active materials were used for the working electrode while lithium was used for the counter and reference electrode. A glass fiber separator was used as the separator membrane. 1 M LiClO<sub>4</sub> was employed as the electrolyte and dissolved in a mixture of EC (ethylene carbonate):PC (propylene carbonate) in a 1:1 volume ratio [17, 19–21].

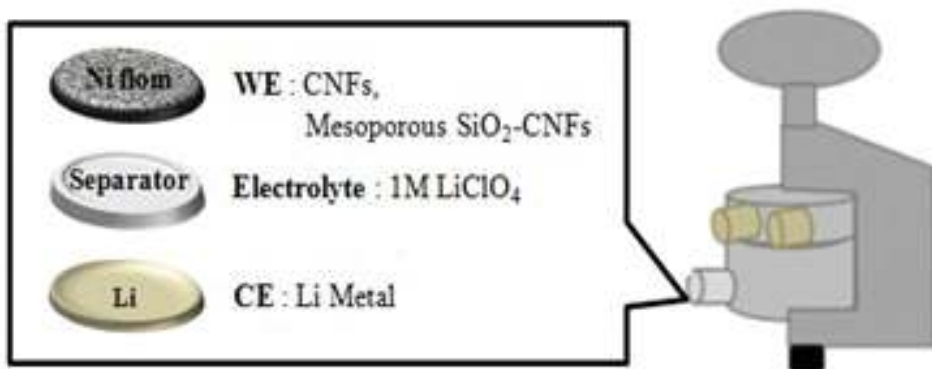


**Figure 8.** Fabrication scheme of lithium secondary batteries.

### 3.1.4. Scanning Electron Microscope (SEM)

SEM images of the CNFs and mesoporous SiO<sub>2</sub>–CNF composites synthesized on Fe–Cu, Fe–Cu/mesoporous SiO<sub>2</sub>, and mesoporous SiO<sub>2</sub>-deposited Ni foam using the CVD method were obtained. Analysis of the SEM images showed that CNFs and mesoporous SiO<sub>2</sub>–CNF composites grew on Fe–Cu, Fe–Cu/mesoporous SiO<sub>2</sub>, and mesoporous SiO<sub>2</sub>-deposited Ni foam. The average diameter of the grown CNFs was 25–100 nm [18] (**Figure 9**).

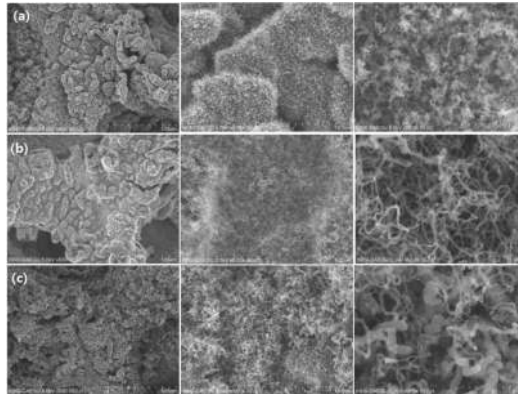


**Figure 9.** SEM images of CNFs and mesoporous SiO<sub>2</sub>-CNF composites. (a) CNF-BF/Fe-Cu/Ni foam, (b) CNF-BF/Fe-Cu/mesoporous SiO<sub>2</sub>/Ni foam, and (c) CNF-BF/mesoporous SiO<sub>2</sub>/Ni foam.

### 3.1.5. Transmission electron microscopy (TEM)

TEM was measured to determine the development of porosity in the synthesized mesoporous SiO<sub>2</sub> materials as well as the structure of the synthesized CNFs and mesoporous SiO<sub>2</sub>-CNF composites. Panel **Figure 10(a)** shows that mesoporous SiO<sub>2</sub> with uniform porosity was synthesized. As shown in **Figure 10(b)**, CNFs were synthesized with a hollow tube-like structure in various diameters. As shown in **Figure 10(c)**, the CNFs were surrounded by mesoporous SiO<sub>2</sub> in the mesoporous SiO<sub>2</sub>-CNF composites. Panel **Figure 10(d)** shows the elemental mapping from analyzing Si and O atoms. The overall distributions of mesoporous silica were examined [18] (**Figure 10**).

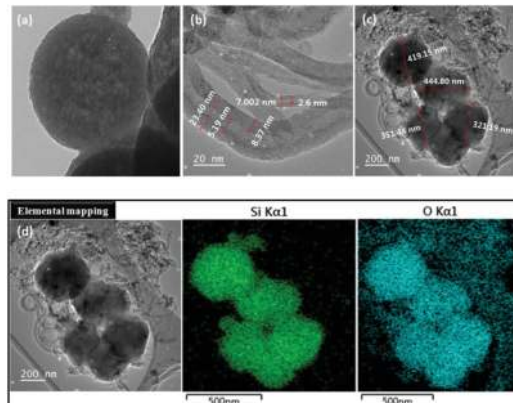


**Figure 10.** TEM images of CNFs and mesoporous SiO<sub>2</sub>-CNF composites. (a) mesoporous SiO<sub>2</sub>, (b) CNF-BF/Fe-Cu/Ni foam, (c) CNF-BF/mesoporous SiO<sub>2</sub>/Ni foam, and (d) elemental mapping of CNF-BF/mesoporous SiO<sub>2</sub>/Ni foam.

### 3.1.6. Cycle performances

Charging–discharging characteristics were examined by employing a current of 100 mA/g in order to investigate electrochemical characteristics such as the capacity and cycle ability of the three-electrode cell synthesized by applying CNFs and the mesoporous SiO<sub>2</sub>–CNF composites synthesized in this study as anode active materials. The electrochemical characteristics of the three-electrode cell were examined with and without the binder.

As shown in **Figure 11(a)**, when CNFs synthesized following the deposition of Fe–Cu catalyst on Ni foam were used as anode active materials, the initial capacity (256 mAh/g) was reduced to 231 mAh/g after 30 cycles, resulting in a retention rate of 90.2%. As shown in **Figure 11(b)**, when mesoporous SiO<sub>2</sub>–CNF composites synthesized after the deposition of Fe–Cu catalyst and mesoporous SiO<sub>2</sub> on Ni foam were used as anode active materials, the initial capacity (289 mAh/g) was reduced to 169 mAh/g after 30 cycles, for a retention rate of 58.5%. As shown in **Figure 11(c)**, when mesoporous SiO<sub>2</sub>–CNF composites synthesized after the deposition of mesoporous SiO<sub>2</sub> on Ni foam were used as anode active materials, the initial capacity (2420 mAh/g) was reduced to 2092 mAh/g after 30 cycles. The retention rate was 86.4%.

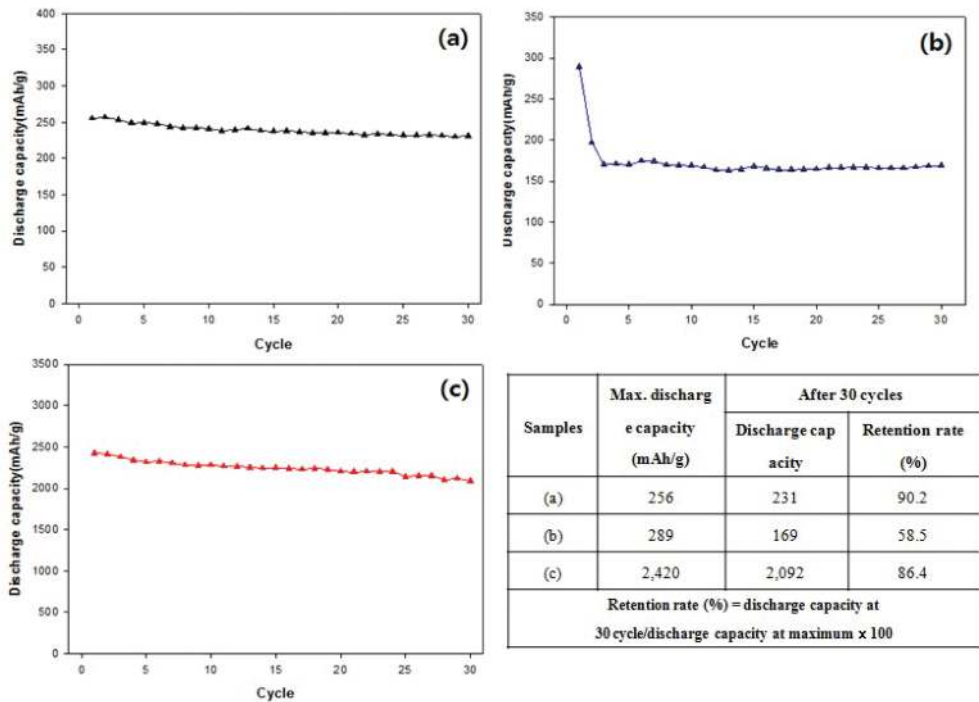


**Figure 11.** Cycle performance of CNFs and mesoporous SiO<sub>2</sub>–CNF composites without binder up to 30 cycles. (a) CNF–BF/Fe–Cu/Ni foam, (b) CNF–BF/Fe–Cu/mesoporous SiO<sub>2</sub>/Ni foam, and (c) CNF–BF/mesoporous SiO<sub>2</sub>/Ni foam.

The discharging capacity of mesoporous  $\text{SiO}_2$ -CNF composites was higher than that of CNFs due to the high theoretical capacity of Si. As shown in (b) and (c), the capacity varied depending on the preparation methods used for mesoporous  $\text{SiO}_2$ -CNF composites. The mesoporous  $\text{SiO}_2$ -CNF composites synthesized after Fe-Cu catalyst and mesoporous  $\text{SiO}_2$  deposited on Ni foam did not show relatively good performance compared to those synthesized without a binder. The reason could be that  $\text{SiO}_2$  could not play a role because more CNFs grew in the presence of the Fe-Cu catalyst.

On the other hand, as shown in **Figure 11(c)**, mesoporous  $\text{SiO}_2$ -CNF composites were synthesized after mesoporous  $\text{SiO}_2$  was deposited on Ni foam without a catalyst. The CNFs grew because the Ni foam served as the catalyst. Thus, panel (c) had a higher capacity due to the mesoporous  $\text{SiO}_2$  than panel **Figure 11(b)**, in which many CNFs were grown. The CNFs also grew appropriately. Thus, the retention rate was relatively high [18] (**Figure 11**).

### 3.2. Synthesis and electrochemical performance of $\text{SiO}_2$ /CNF composite on Ni-Cu/C-fiber textiles

#### 3.2.1. Deposition of catalysts

The electrophoretic deposition method was used to deposit Ni and Cu catalysts onto C-fiber textiles, and a schematic diagram of the experimental apparatus used in electrophoretic deposition is displayed in **Figure 12**. The C-fiber textiles were used as the cathode and a carbon electrode was employed as an anode, with a distance of 85 mm between each electrode. Three experimental conditions were employed in depositing the catalyst onto the C-fiber textiles. Ni was deposited onto the C-fiber textiles with a nickel(II) acetate tetrahydrate aqueous solution (Ni) while Ni and Cu were deposited onto the C-fiber textiles with a mixed solution of nickel(II) acetate tetrahydrate and copper(II) acetate monohydrate (Ni-Cu). For the third condition, Cu

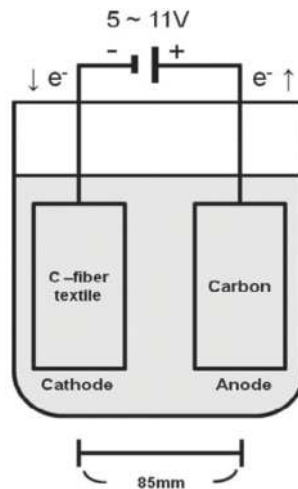


**Figure 12.** Electrophoretic deposition apparatus used in the deposition of catalysts.

was predeposited onto the C-fiber textiles and Ni was subsequently deposited onto the same C-fiber textile in a nickel(II) acetate tetrahydrate aqueous solution (Ni/Cu) [11, 14, 16, 22, 23].

### 3.2.2. Reduction

A reduction step was applied. This was done to convert the metal oxides on the surface of the C-fiber textiles into elemental nickel and copper using a tube furnace. H<sub>2</sub> gas mixed with N<sub>2</sub> gas was used for the reduction process, and the flux of the reaction gas was regulated by MFC. The reactor temperature was increased at the rate of 12°C/min, until it reached 700°C. Once the temperature reached 700°C, N<sub>2</sub> gas mixed with 20% H<sub>2</sub> gas was flowed into the reactor. This reduction process was performed for 2 h [23, 24].

### 3.2.3. Growth of CNFs

CNFs were synthesized onto C-fiber textiles using the CVD method in a horizontal tube furnace after the reduction process was completed. The prepared metal catalyst was evenly spread on a quartz boat, which was then placed into the reactor under an N<sub>2</sub> atmosphere, and the reactor temperature was increased to 12°C/min. Once the temperature reached 700°C, this temperature was maintained for 30 min; 20% H<sub>2</sub> gas balanced with N<sub>2</sub> gas was flowed into the reactor. Then, for 3 h, the H<sub>2</sub> gas balanced with N<sub>2</sub> gas and 20% ethylene balanced with N<sub>2</sub> gas were flowed together into the reactor. The flow of ethylene and H<sub>2</sub> gases was cut off after the reaction was completed. N<sub>2</sub> was then passed through the reactor under an inactive reactor atmosphere to cool it down to room temperature [23, 24].

### 3.2.4. Oxidation and SiO<sub>2</sub> coating on CNFs

For SiO<sub>2</sub> coating on the surface of CNFs, the hydroxyl group was introduced as an anchor group. This was performed by oxidizing the hydroxyl group for half an hour in 80°C nitric acid and rinsing with distilled water. Then, for the synthesis of a composite of SiO<sub>2</sub>-coated CNFs, TEOS was dissolved in ethyl alcohol followed by the dispersion of the CNFs grown on C-fiber textiles in the solution and addition of ammonia water for a 24 h reaction at 50°C [23, 24].

### 3.2.5. Fabrication of anode materials for lithium secondary batteries

The as-prepared CNFs were grown on C-fiber textiles without any binders and the conducting compounds were used as working electrodes for the fabrication of a conventional three-electrode cell. Lithium was used as the counter and reference electrode. A glass fiber separator was used as the separator membrane. 1 M LiClO<sub>4</sub> was employed as the electrolyte and dissolved in a mixture of EC (ethylene carbonate):PC (propylene carbonate) in a 1:1 volume ratio [23].

### 3.2.6 Scanning Electron Microscope (SEM)

SEM images of CNFs grown with the Ni (a), Ni–Cu (b), and Ni/Cu (c) catalysts deposited onto C-fiber textiles are shown in **Figure 13**. As shown in **Figure 13(a)**, Y-shaped CNFs were grown with an average diameter of 40 nm using the Ni catalyst only, representing the growth of CNF

branches that stem from a single origin. Meanwhile, in **Figure 13(b)**, another type of Y-shaped CNFs stemming from a single catalyst in various directions is shown. This figure is relevant to the size of the catalysts created because of the differences in the average diameters. Furthermore, in **Figure 13(c)**, helically grown CNFs with a uniform diameter of 33 nm are shown. With Ni deposited onto the predeposited C-fiber textiles, no Y-shaped carbon nanofiber can be observed in **Figure 13(c)** due to the tendency of the catalyst deposit and the introduction of Cu to affect the growth mechanism of CNFs [23].

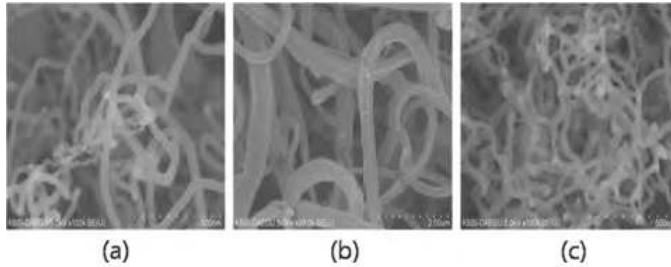


**Figure 13.** SEM images of CNFs grown on the catalysts Ni (a), Ni-Cu (b), and Ni/Cu (c) on C-fiber textiles.

### 3.2.7. Transmission electron microscopy (TEM)

TEM images were analyzed in order to investigate the structure of the  $\text{SiO}_2$ -coated layer in the  $\text{SiO}_2$ /CNF composite after the growth of CNFs onto C-fiber textiles. These images are shown

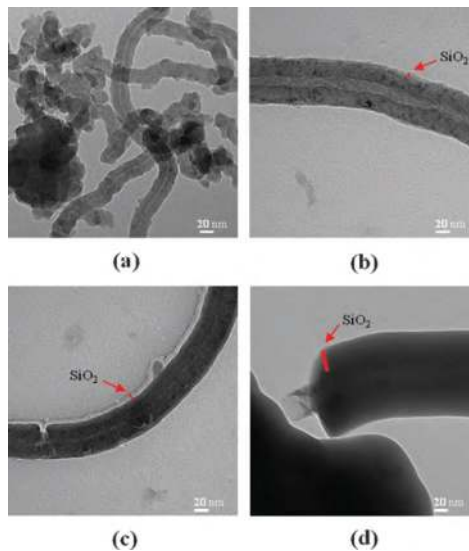


**Figure 14.** TEM images of CNFs (a) and  $\text{SiO}_2$ /CNF composite (b)–(d).

in **Figure 14**. As shown in **Figure 14(a)**, the TEM image of CNFs illustrates the multilayer graphite forming wires with a central microhollow. As for the TEM images from the  $\text{SiO}_2/\text{CNF}$  composite **Figure 14(b)–(d)**, they represent the  $\text{SiO}_2$  from the output of TEOS hydrolysis, which was uniformly coated onto the CNFs to obtain a layered structure [23, 24].

### 3.2.8. Cycle performances

The  $\text{SiO}_2/\text{CNF}$  composite was subjected to a repeated cycling test at a current density of  $100 \text{ mA g}^{-1}$  within a voltage window of 0.1–2.6 V. For comparison, the CNF electrode was tested at the same condition. The cycling performances of the CNFs and the  $\text{SiO}_2/\text{CNF}$  composite electrodes for Li secondary batteries are shown in **Figure 15**. The early-stage discharge capacity of the CNF electrode was  $300 \text{ mAh/g}$  and a near-stable discharge capacity was maintained for 30 cycles. In the case of the  $\text{SiO}_2/\text{CNF}$  composite, a comparatively high discharge capacity of  $2053 \text{ mAh/g}$  was observed in the second cycle, and the discharge capacity of the 29th cycle was significantly reduced to  $1295 \text{ mAh/g}$ , with 63% capacity retention as compared to that of the second cycle. This indicates that the discharge capacity of the CNF electrode nearly reached its theoretical capacity ( $372 \text{ mAh/g}$ ) and showed no decline. The  $\text{SiO}_2/\text{CNF}$  composite had a high discharge capacity of  $2053 \text{ mAh/g}$ , but the cycle performance was not as good as that of the CNFs [23].

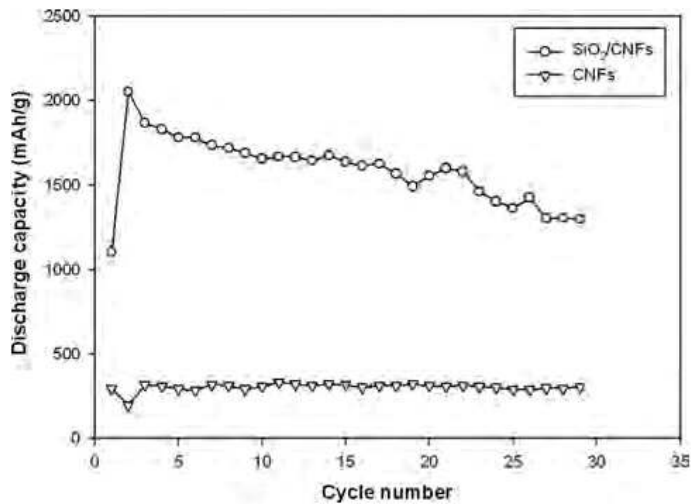


**Figure 15.** Discharge capacity of CNFs and  $\text{SiO}_2/\text{CNF}$  composite.

## 4. Conclusions

CNFs were synthesized by using CVD and the effects of synthesis conditions on the growth of CNFs were investigated by controlling the synthesis temperature and the concentration ratio

of transition metal catalysts. Physiochemical and electrochemical characteristics of the grown CNFs were investigated using various spectroscopic and electrochemical techniques. Based on these CNFs, SiO<sub>2</sub>-CNF composites were synthesized, and the physiochemical characteristics of the SiO<sub>2</sub>/CNF composites as well as their electrochemical characteristics as anode materials of lithium secondary batteries were investigated.

- (1) CNFs were synthesized by ethylene decomposition using CVD based on Fe and Cu catalysts. According to the SEM measurements, the CNFs had 15–35 nm diameter. In addition, according to the measured specific surface areas (m<sup>2</sup>/g) of carbon nanofibers using BET, the synthesized CNFs had the largest specific surface area of 77–305 m<sup>2</sup>/g [9, 11].
- (2) CNFs were synthesized by ethylene decomposition using CVD with Co and Cu catalysts. According to the SEM measurements, the CNFs had 20–35 nm diameter. In addition, according to the measured specific surface areas (m<sup>2</sup>/g) of the carbon nanofibers using BET, the synthesized CNFs had the largest specific surface area of 178–306 m<sup>2</sup>/g [11, 14].
- (3) CNFs and mesoporous SiO<sub>2</sub>-CNF composites were synthesized using Fe-Cu binary catalysts with the CVD method. According to the results of SEM measurements, the average diameter of grown CNFs along with mesoporous SiO<sub>2</sub> was 25–100 nm. According to the results of galvanostatic charging and discharging, the discharging capacity of mesoporous SiO<sub>2</sub>-CNF composites was higher than that of CNFs due to the high theoretical capacity of Si. In particular, mesoporous SiO<sub>2</sub>-CNF composites synthesized without binders after mesoporous SiO<sub>2</sub> was deposited on Ni foam showed the highest charging and discharging capacity and retention rate. The initial capacity (2420 mAh/g) was reduced to 2092 mAh/g after 30 cycles for a retention rate of 86.4% [18].
- (4) CNFs were grown with the CVD method onto C-fiber textiles, based upon Ni, Ni-Cu, and Ni/Cu catalysts, followed by TEOS hydrolysis to coat SiO<sub>2</sub> onto the CNFs. The conclusion of the results is as follows. CNFs grown on Ni/C-fiber textiles were synthesized with a diameter of 40 nm and showed a consistent Y-shaped branch morphology. CNFs grown on Ni-Cu/C-fiber textiles were synthesized with a diameter of 300 nm and had a multidirectional Y-shaped branch morphology. CNFs grown on Ni/Cu/C-fiber textiles appeared to be the most uniform CNFs and had a diameter of 33 nm. Based on galvanostatic charge-discharge, the SiO<sub>2</sub>/CNF composites featured a much more excellent discharge capacity of 1295 mAh/g compared to the CNF, which remained at 304 mAh/g, after 29 cycles. Further, a fairly decent capacity retention, 63% compared to the first two cycles, was observed after 20 cycles [23].

## Acknowledgements

This research was financially supported by the Ministry of Education, Science Technology (MEST) and National Research Foundation of Korea (NRF) through the Human Resource Training Project for Regional Innovation (No. 2015035858).



## Author details

Chang-Seop Lee\* and Yura Hyun

\*Address all correspondence to: [surfkm@kmu.ac.kr](mailto:surfkm@kmu.ac.kr)

Department of Chemistry, Keimyung University, Daegu, South Korea

## References

- [1] Peter M. Martin, editor. Handbook of Deposition Technologies for Films and Coatings: Science, Applications and Technology. 3rd ed. UK: Elsevier; 2009. pp. 400–459.
- [2] Jong-Hee Park, T.S. Sudarshan, editor. Chemical Vapor Deposition. 1st ed. USA: ASM International; 2001. pp. 1–22.
- [3] Jinbo Bai, Aïssa Allaoui, Effect of the length and the aggregate size of MWNTs on the improvement efficiency of the mechanical and electrical properties of nanocomposites – experimental investigation. 2003;34(8):689. DOI:10.1016/S1359-835X(03)00140-4
- [4] Orna Breuer, Uttandaraman Sundararaj. Big Returns from Small Fibers: A Review of Polymer/Carbon Nanotube Composites. Polymer Composites. 2004;25(6):630–645. DOI: 10.1002/pc.20058
- [5] Jae-Seok Lim, Seong-Young Lee, Sei-Min Park, Myung-Soo Kim. Preparation of Carbon Nanofibers by Catalytic CVD and Their Purification. Carbon Letters. 2005;6(1):31–40.
- [6] Krijn P. de Jong, John W. Geus. Carbon Nanofibers: Catalytic Synthesis and Applications. Catalysis Reviews: Science and Engineering. 2000;42(4):481–510. DOI: 10.1081/CR-100101954
- [7] Taeyun Kim, Karina Mees, Ho-Seon Park, Monika Willert-Porada, Chang-Seop Lee. Growth of Carbon Nanofibers Using Resol-Type Phenolic Resin and Cobalt(II) Catalyst. Journal of Nanoscience and Nanotechnology. 2013;13(11):7337–348. DOI: <http://dx.doi.org/10.1166/jnn.2013.7852>
- [8] Jia-Qi Huang, Wancheng Zhu, Ling Hu, Qiang Zhang, Fei Wei. Robust Growth of Herringbone Carbon Nanofibers on Layered Double Hydroxide Derived Catalysts and Their Applications as Anodes for Li-ion Batteries. Carbon. 2013;62:393–404. DOI: 10.1016/j.carbon.2013.06.023
- [9] Yura Hyun, Haesik Kim, Chang-Seop Lee. Synthesis of Carbon Nanofibers on Iron and Copper Catalysts by Chemical Vapour Deposition. Advanced Materials Research. 2013;750–752:265–275. DOI: 10.4028/www.scientific.net/AMR.750-752.265
- [10] Taeyun Kim, Hosun Park, Monica Willert Porada, Chang-Seop Lee. Growth of Carbon Nanofibers Using Resol-Type Phenolic Resin and Cobalt(II) Catalyst. Journal of

- Nanoscience and Nanotechnology. 2013;13(11):7337–7348. DOI: <http://dx.doi.org/10.1166/jnn.2013.7852>
- [11] Yura Hyun, Eun-Sil Park, Karina Mees, Ho-Seon Park, Monika Willert-Porada, Chang-Seop Lee. Synthesis and Characterization of Carbon Nanofibers on Transition Metal Catalysts by Chemical Vapour Deposition. *Journal of Nanoscience and Nanotechnology*. 2015;15(9):7293–7304. DOI: <http://dx.doi.org/10.1166/jnn.2015.10588>
- [12] Eun-Sil Park, Jong-Ha Choi, Chang-Seop Lee. Synthesis and Characterization of Vapor-grown Si/CNF and Si/PC/CNF Composites Based on Co–Cu Catalysts. *Bulletin of the Korean Chemical Society*. 2015;36(5):1366–1372. DOI: 10.1002/bkcs.10262
- [13] Eunyi-Jang, Heai-Ku Park, Jong-Ha Choi, Chang-Seop Lee. Synthesis and Characterization of Carbon Nanofibers Grown on Ni and Mo Catalysts by Chemical Vapor Deposition. *Bulletin of the Korean Chemical Society*. 2015;36(5):1452–1459. DOI: 10.1002/bkcs.10285
- [14] Eun-Sil Park, Jong-Won Kim, Chang-Seop Lee, Synthesis and Characterization of Carbon Nanofibers on Co and Cu Catalysts by Chemical Vapor Deposition. *Bulletin of the Korean Chemical Society*. 2014;35(6):1687–1695. DOI : 10.5012/bkcs.2014.35.6.1687
- [15] Sang-Won Lee, Chang-Seop Lee. Growth and Characterization of Carbon Nanofibers on Fe/C-fiber Textiles Coated by Deposition-Precipitation and Dip-Coating. *Journal of Nanoscience and Nanotechnology*. 2015;15(9):7317–7326. DOI: <http://dx.doi.org/10.1166/jnn.2015.10585>
- [16] Sang-Won Lee, Chang-Seop Lee. Electrophoretic Deposition of Iron Catalyst on C-Fiber Textiles for the Growth of Carbon Nanofibers. *Journal of Nanoscience and Nanotechnology*. 2014;14(11): 8619–8625. DOI: <http://dx.doi.org/10.1166/jnn.2014.9960>
- [17] Yura Hyun, Heai-Ku Park, Ho-Seon Park, Chang-Seop Lee. Characteristics and Electrochemical Performance of Si-Carbon Nanofibers Composite as Anode Material for Binder-Free Lithium Secondary Batteries. *Journal of Nanoscience and Nanotechnology*. 2015;15(11):8951–8960. DOI: <http://dx.doi.org/10.1166/jnn.2015.11553>
- [18] Yura Hyun, Jin-Yeong Choi, Heai-Ku Park, Jae Young Bae, Chang-Seop Lee. Synthesis and Electrochemical Performance of Mesoporous SiO<sub>2</sub>-Carbon Nanofiber Composite as Anode Materials for Lithium Secondary Batteries. *Materials Research Bulletin*. Forthcoming.
- [19] Eun-Sil Park, Heai-Ku Park, Ho-Seon Park, Chang-Seop Lee. Synthesis and Electrochemical Properties of CNF–Si Composites as an Anode Material for Li Secondary Batteries. *Journal of Nanoscience and Nanotechnology*. 2015;15(11):8961–8970. DOI: <http://dx.doi.org/10.1166/jnn.2015.11554>
- [20] Eunyi-Jang, Heai-Ku Park, Chang-Seop Lee. Synthesis and Application of Si/Carbon Nanofiber Composites based on Ni and Mo Catalysts for Anode Material of Lithium

- Secondary Batteries. *Journal of Nanoscience and Nanotechnology*. Forthcoming. DOI: 10.1166/jnn.2016.12229
- [21] Yura Hyun, Jin-Young Choi, Heai-Ku Park, Chang-Seop Lee. Synthesis and Electrochemical Performance of Ruthenium Oxide-coated Carbon Nanofibers as Anode Materials for Lithium Secondary Batteries. *Applied Surface Science*. Forthcoming. DOI: <http://dx.doi.org/10.1016/j.apsusc.2016.01.095>
- [22] Sang-Won Lee, Karina Mees, Ho-Seon Park, Monika Willert-Porada, Chang-Seop Lee. Synthesis of Carbon Nanofibers on C-fiber Textiles by Thermal CVD Using Fe Catalyst. *Advanced Materials Research*. 2013;750–752:280–292. DOI: 10.4028/www.scientific.net/AMR.750–752.280
- [23] Ki-Mok Nam, Heai-Ku Park, Chang-Seop Lee. Synthesis and Electrochemical Properties of Carbon Nanofibers and SiO<sub>2</sub>/Carbon Nanofiber Composite on Ni-Cu/C-Fiber Textiles. *Journal of Nanoscience and Nanotechnology*. 2015;15(11):8989–8995. DOI: <http://dx.doi.org/10.1166/jnn.2015.11555>
- [24] Ki-Mok Nam, Karina Mees, Ho-Seon Park, Monika Willert-Porada, Chang-Seop Lee. Electrophoretic Deposition for the Growth of Carbon Nanofibers on Ni-Cu/C-fiber Textiles. *Bulletin of the Korean Chemical Society*. 2014;35(8):243–2437. DOI: <http://dx.doi.org/10.5012/bkcs.2014.35.8.2431>

